S. V. Kozhevnikov^{a,b}, V. K. Ignatovich^a, F. Ott^{c,d},
A. Rühm^b, J. Major^b

EXPERIMENTAL DETERMINATION
OF THE NEUTRON CHANNELING LENGTH
IN A PLANAR WAVEGUIDE

^{a} Joint Institute for Nuclear Research, Dubna
^{b} Max-Planck-Institut für Intelligente Systeme (formerly Max-Planck-Institut
für Metallforschung), Stuttgart, Germany
^{c} CEA, IRAMIS, Laboratoire Léon Brillouin, Gif sur Yvette, France
^{d} CNRS, IRAMIS, Laboratoire Léon Brillouin, Gif sur Yvette, France

Кожевников С. В. и др.   E14-2012-117

Экспериментальное определение длины каналирования
нейтронов в плоском волноводе

В нейтронных волноводах нейтронная волна удерживается внутри волноводного слоя и может выходить из торца слоя в виде микропучка. Каналирование внутри волноводного слоя сопровождается экспоненциальным затуханием плотности волновой функции нейтронов внутри волновода. Мы напрямую определили соответствующий параметр затухания, называемый длиной каналирования. Для этого мы измеряли интенсивность микропучка как функцию длины поглощающего нейтроны материала, помещённого на поверхность волновода. Такие плоские волноводы преобразуют обычный нейтронный пучок в предельно узкий, но немного расходящийся микропучок, который может использоваться для исследования наноструктур с субмикронным пространственным разрешением.

Kozhevnikov S. V. et al.   E14-2012-117

Experimental Determination of Neutron Channeling
Length in a Planar Waveguide

In neutron waveguides the neutron wave is confined inside the guiding layer of the structure and can escape from the layer edge as a microbeam. The channeling within the guiding layer is accompanied by an exponential decay of the neutron wave function density inside the waveguide. Here we report direct determination of the corresponding decay constant, termed neutron channeling length. For this, we measured the microbeam intensity as a function of the length of a neutron absorbing layer of variable length placed onto the surface of a waveguide structure. Such planar neutron waveguides transform a conventional neutron beam into an extremely narrow but slightly divergent microbeam which could be used for the investigation of nanostructures with submicron spatial resolution.

Neutron scattering is a powerful tool for the investigation of magnetic structures, polymers, and biological objects. The information obtained about the investigated systems is, however, averaged over the neutron beam width which is usually of the order of 0.1 to 10 mm. For investigation of nanostructures with high spatial resolution, focusing devices (such as focusing crystal monochromators or focusing guides) have been developed, which may focus the neutron beam in one or two dimensions. However, these devices are restricted by their physical properties and manufacturing technologies and cannot produce beam focus of less than 50 μm width [1]. Potential devices for the production of submicron neutron beams in one dimension are layered planar waveguides which transform a conventional neutron beam into an extremely narrow (< 1 μm), although slightly divergent ($0.1°$) neutron microbeam emerging from the edge of a waveguide [2–5].

The phenomenon of neutron channeling in planar waveguides was observed experimentally in [6–9], but the value of the neutron channeling length (CL) was never measured. In this communication we present a direct measurement of this CL and compare it with the theory [10]. Note that the case of neutrons is significantly different from the case of X-rays because the neutron absorption is very weak compared to X-rays. The absorption length of 4 Å neutrons in copper is 7.2 mm while it is 22 μm for 8 keV X-rays. The absorption is thus not the main parameter defining the value of the CL, and this makes a direct measurement feasible.

The problem of neutron propagation at interfaces was already studied earlier. We can, for example, mention the attempts to measure the Goos–Hönchen (GH) effect during the reflection of a neutron on a surface [11]. In the GH effect, the neutron propagates along the surface in the form of an evanescent wave. In the case of waveguides, it propagates in the form of resonant modes. In such a situation, the propagation length can be enhanced by several orders of magnitude making the measurement technically feasible.

Let us consider a waveguide structure of the type Fe(10 nm)/Cu(150 nm)/Fe(50 nm)//glass. In such a structure, resonant modes characterized by a quantum number n are excited in the guiding Cu layer for specific incidence angles [2]. Figure 1 shows the propagation of the resonance mode $n = 2$ for neutron of spin up inside the guiding layer which takes place over 100 μm. The propagation length may be further increased by selecting a lower order mode, by increasing the thickness of the top Fe coupling layer, the thickness of the guiding layer, the
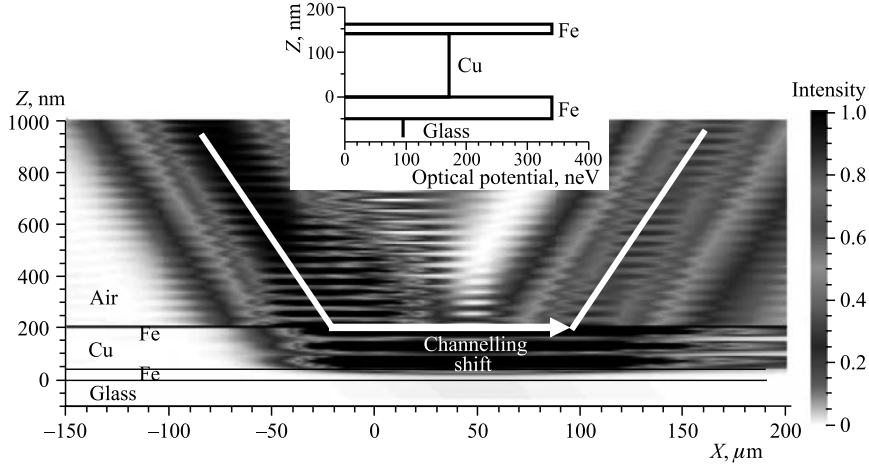
Fig. 1. Propagation of the neutron wave inside a Fe(10 nm)/Cu(150 nm)/Fe(50 nm)//glass waveguide structure. Neutron-optical potential inside the waveguide (inset)
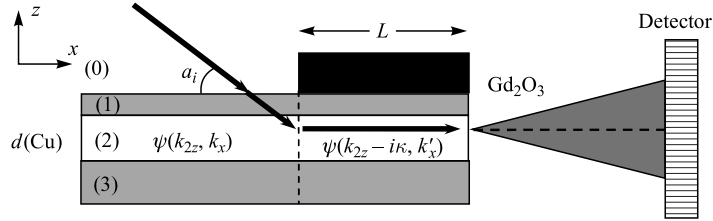

Fig. 2. Experimental setup. The waveguide is covered with an absorber of variable length L at its end

potential well depth or by increasing the coherence (lowering the divergence) of the incident beam. This is not shown because the corresponding figures are far less legible. In optimal conditions it is possible to reach mm size length scales.

A specific geometry can be considered where the resonant mode propagates along the channel and eventually exits the channel edge (Fig. 2). If part of the sample surface above the channel is shielded from the incident wave (Fig. 2), we will show that the wave field exponentially decreases along the channel $\sim \exp\left(-x/x_e\right)$, where x_e is the CL.

An analytical description of the neutron resonances in layered structures can be found in [10, 12]. Let us consider a neutron plane wave with the wave vector $\mathbf{k}_0$ incident on the structure of Fig. 2 with a grazing angle α_i. The wave function

2

in the resonant layer can be represented as

$$\psi(r) = A\,e^{ik_{0x}x}\left(e^{-ik_{2z}z} + R_{23}\,e^{ik_{2z}z}\right),\tag{1}$$

where $k_{2z} = \sqrt{k_{0z}^2 - u_{\mathrm{Cu}}}$ is the z component of the neutron wave vector inside the guiding Cu layer; u_{Cu} is the optical potential of the Cu layer; R_{23} is the reflection amplitude from the bottom Fe barrier (3) within the Cu layer (2), and the point $z = 0$ coincides with the interface of the bottom Fe layer. The factor A is the amplitude of the wave incident on the bottom Fe layer. It is determined from the self-consistent equation [12]:

$$A = T_{02}\,\exp\left(ik_2 d\right) + R_{21}R_{23}\,\exp\left(2ik_2 d\right)A,\tag{2}$$

where T_{02} is the transmission amplitude through the top Fe barrier from vacuum (0) into the Cu layer (2), and R_{21} is the reflection amplitude within Cu (2) from the top Fe barrier (1). It follows from (2) that

$$|A| = |T_{02}|/|1 - R_{21}R_{23}\,\exp\left(2ik_{2z}d\right)|,\tag{3}$$

so the A has maxima at resonances $k_{0z} = k_0\sin\alpha_n$, satisfying the equation

$$\gamma(k_{0z}) = 2k_{2z}d + \arg\left(R_{21}\right) + \arg\left(R_{23}\right) = 2\pi n.\tag{4}$$

The neutron wave function under the nonilluminated section of the waveguide can be represented by the product $Z(z)X(x)$, as in (1). The $Z(z)$ part:

$$Z(z) = A(e^{-ik'_{2z}z} + R_{23}\,e^{ik'_{2z}z}),\tag{5}$$

should not change along the channel, and $X(x) = \exp\left(ik'_x x\right)$. The amplitude A in (5) should be the same as in the illuminated part, but k_{2z} should acquire a negative imaginary part $k'_{2z} = k_{2z} - i\kappa$ in the nonilluminated part of the channel. Without this imaginary part, the function $Z(z)$ cannot stay the same in the shadowed region. Indeed, the wave $e^{-ik'_{2z}z}$ after reflection from the bottom layer, propagation to the top layer, and coming back to the bottom layer acquires the amplitude $R_{23}R_{21}\,e^{2ik'_{2z}d}$. If we want this amplitude to remain unity as at the start, it requires $R_{23}R_{21}\,e^{2ik'_{2z}d} = 1$, from which it follows that the real part of k'_{2z} should be equal to k_{2z}. To satisfy the resonance condition (4), the imaginary part should be $\kappa = -\ln|R_{21}R_{23}|/2d$ to compensate the losses because of transmissions through both Fe layers. If the thicknesses of the two Fe layers in Fig.1 are large enough, then $|R_{21}R_{23}| \approx 1$ and κ is small.

To find the propagation wave vector k'_x in the channel under the nonilluminated area one has to apply the law of energy conservation

$$(k_{2z} - i\kappa)^2 + k'^2_x = k_{2z}^2 + k_x^2\tag{6}$$

from which it follows that

$$k'_x = \sqrt{k_x^2 + 2i\kappa k_{2z}} \approx k_x + i\kappa k_{2z}/k_x. \tag{7}$$

The imaginary part of k'_x is positive, which leads to $X(x) = \mathrm{e}^{ik'_x x} = \mathrm{e}^{ik_x^x - x/2x_e}$ and thus to the exponential decay of the intensity $I \propto \exp\left(-x/x_e\right)$ with the CL

$$x_e = k_x/2\kappa k_{2z} \approx k_x d/k_{2z} \left|\ln|R_{21}R_{23}|\right|. \tag{8}$$

The investigated waveguide structure was Fe(200 Å)/Cu(1400 Å)/Fe(500 Å)// glass(substrate) with magnetically saturated Fe layers. This system in the case of fully magnetized Fe state represents a potential well between two high potential barriers for neutrons polarized parallel to the Fe magnetization. Inside the guiding layer, the neutron wave function at the resonance $n = 0$ has an amplitude $A = 17.1$ comparing to unity of the incident wave amplitude. In the following, we will discuss our results on neutron channeling at the resonance $n = 0$, which is characterized by the highest neutron wave-function amplitude.

The experiment was carried out at the polarized neutron reflectometer N-REX$^+$ (Forschungsneutronenquelle Heinz Maier-Leibnitz, FRM II, Garching, Germany) with the surface of the waveguide sample oriented horizontally. The neutron wavelength was 4.26 Å (FWHM = 1%), the incidence angle resolution was 0.006°. Magnetized supermirrors in transmission mode were used as neutron spin polarizer and analyzer. The polarization of the incident beam was 97%, and the polarizing efficiency of the analyzer was 94%. A Mezei-type spin-flipper of 100% efficiency was used to flip the polarization of the incident beam. The reflectivity of the waveguide structure was measured using a two-dimensional position-sensitive ^{3}He gas detector with a spatial resolution of 3 mm (FWHM). The distance between the collimating diaphragm and the waveguide sample was 2200 mm, the sample-detector distance was 2500 mm. As an absorber we used Gd_2O_3 powder with a grain size of about 1 μm, so that the optical properties of the waveguide were not altered by the absorber. The height of the applied Gd_2O_3 powder was 2–3 mm which was sufficient to absorb the reflected beam. The dry powder was carefully put by hand onto the sample surface according to the desired length L of the coverage.

The sample size was $30 \times 30 \times 5$ mm^3. The sample structure as determined from specular reflectivity [4] was FeO(54Å)/Fe(154Å)/Cu(1360Å)/Fe(510Å)//glass (substrate). Waveguide resonance was experimentally found in [4] at the incidence angle $\alpha_0 = 0.37°$, which is in good agreement with theoretical values, Eq. (5): $\alpha_0 = 0.365°$.

The neutron microbeam intensity measured for *up* polarization of the incident beam near the resonance $n = 0$ is shown in Fig. 3 as a function of the incidence angle α_i for different absorber lengths L. This microbeam intensity was determined by integration over a narrow interval of outgoing angles ($\pm 0.1°$) around

the sample horizon which was defined by the analyzer aperture. The microbeam intensity without any absorber coverage ($L = 0$) is accompanied by a high level of background arising from the specularly reflected beam. The background level for practically any minute length of the absorber coverage is much lower due to the blocking of the reflected beam by the macroscopic barrier of Gd_2O powder.

The angular positions of the peaks in the microbeam intensity shown in the four panels of Fig. 3 are not exactly identical due to slightly different experimental off-sets in the incidence-angles scales. The sample was removed and placed back after each measurement to change the absorber length. Afterwards the angular off-set was not checked and revised since the specularly reflected beam was blocked by the absorber. For the purpose of this article, however, the absolute peak positions are not needed.
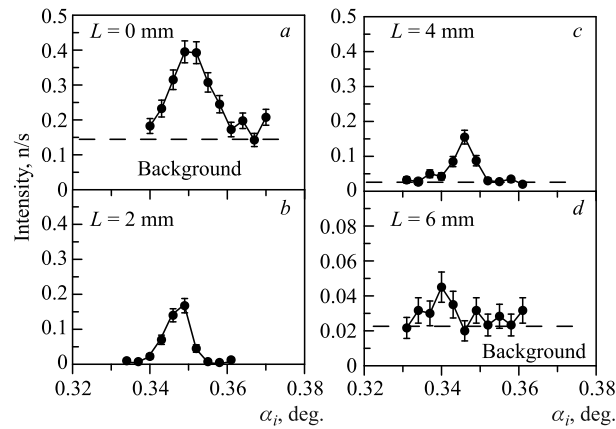

Fig. 3. Neutron microbeam intensity as a function of the incidence angle a_i for different length of the absorbing Gd_2O_3 powder layer (see Fig. 2). The incidence-angle scales are slightly shifted with respect to each other since the sample was remounted for each measurement (see the main text). The dashed line marks the background level
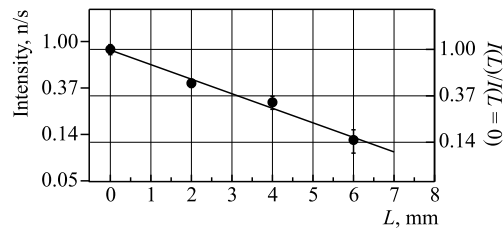

Fig. 4. Microbeam intensity (after background subtraction) as a function of the absorber length L in natural logarithmic ordinate scale

The integrated-peak area $I(x)$ of the microbeam intensities displayed in Fig. 3 is plotted as a function of the absorber length L in Fig. 4 with logarithmic ordinate scales. The left ordinate axis represents absolute neutron intensities after background subtraction, with the background level defined by the intensity outside the resonance (marked by dashed lines in Fig. 3). The right ordinate axis represents neutron intensities relative to the intensity without absorber ($L = 0$). An exponential fit to the data yields $x_e = (3.2 \pm 0.3)$ mm for the neutron channeling length, with the error margin estimated from the statistical experimental errors. This result is in good agreement with theoretical value 3.14 mm obtained from (8). This good agreement shows that our waveguide is of very good quality. Other than tunneling through the upper coupling layer loss mechanisms, scattering losses due to interface roughness or bulk inhomogeneities turn out to be negligible for the investigated waveguide.

Our results show that it is possible to efficiently couple a beam of width $x_e \cdot \sin(\alpha_0) \sim 20$ μm into the waveguide and to carry it to the edge of the guiding layer of thickness 1400 Å. This corresponds to a spatial compression ratio higher than 100 (in one direction). Compared to other focusing systems providing also very high compression ratios (such as compound refractive lenses [1]), the layered planar waveguide discussed here has the advantage of producing a very clean microbeam. The use of a planar waveguide allows one to effectively extract a microbeam from the direct and reflected beams. Using absorbers, a better signal to noise ratio can be obtained (compare Fig. 3, a and Fig. 3, b).

Polarized neutron microbeams could be practically used for the investigation of magnetic nanostructures with high spatial resolution in one dimension. In particular this opens possibilities for studying of magnetic microstructures either by direct precession techniques [13, 14] or by phase imaging [15]. Resonant beam couplers may also be used for the production of very high resolution long wavelengths monochromators [16].

In conclusion, we have reported the experimental determination of the neutron channeling length in a planar waveguide structure. The intensity of the neutron microbeam emerging from the edge of the waveguide was recorded as a function of the absorber length at the waveguide surface, which defines the nonilluminated area. The observed decay length agrees well with the theoretical prediction (8). This knowledge should allow one to optimize neutron waveguide structures.

We furthermore expect that the described method to determine the channeling length can be used to characterize imperfections in waveguides via the associated drop of the channeling length. This experimental method can thus contribute to the further development of the theory of channeling in waveguides and to the development of optimized devices for the production of neutron microbeams for the characterization of nanostructures. The method may also more generally prove to be useful as a sensitive tool to characterize chemical, structural, and magnetic imperfections in thin layered structures.

REFERENCES

1. *Ott F.* Focusing Optics for Neutrons. Modern Developments in X-Ray and Neutron Optics // Springer Series in Optical Sciences. 2008. V. 137. P. 113–134.

2. *Pfeiffer F. et al.* // Phys. Rev. Lett. 2002. V. 88. P. 055507.

3. *Pfeiffer F. et al.* // Proc. SPIE. 2001. V. 4509. P. 79.

4. *Kozhevnikov S. V. et al.* // Physica B. 2011. V. 406. P. 2463.

5. *Kozhevnikov S. V., Rühm A., Major J.* // Crystallogr. Rep. 2011. V. 56. P. 1207.

6. *Feng Y. P. et al.* // Phys. Rev. B. 1994. V. 49. P. 10814.

7. *Pogossian S. P. et al.* // Phys. Rev. B. 1996. V. 53. P. 14359.

8. *Menelle A. et al.* // Physica B. 1997. V. 234–236. P. 510.

9. *Aksenov V. L., Nikitenko Yu. V.* // Physica B. 2001. V. 297. P. 101.

10. *Ignatovich V. K., Radu F.* // Phys. Rev. B. 2001. V. 64. P. 205408.

11. *de Haan V. O. et al.* // Phys. Rev. Lett. 2010. V. 104. P. 010401;
    Ignatovich V.K. // Comment, Phys. Rev. Lett. 2010. V. 105. P. 018901.

12. *Radu F., Ignatovich V. K.* // Physica B. 2000. V. 292. P. 160.

13. *Thibaudeau P. et al.* // Europhys. Lett. 2011. V. 93. P. 3700.

14. *Kozhevnikov S. V. et al.* Use of Waveguides for Polarized Neutron Studies at the Micrometric Scale // Jornal of Instrumentation (submitted). http://arxiv.org/abs/1209.3889.

15. *Krüger S. P. et al.* // J. Synchrotron Radiation. 2012. V. 19. P. 227.

16. *Feng Y. P. et al.* // Phys. Rev. Lett. 1993. V. 71. P. 537.

Редактор *Э. В. Ивашкевич*